Reactive Processing Compatibilization of Direct Injection Molded Polyamide-6/Poly(Ethylene Terephthalate) Blends

A. Retolaza, J. I. Eguiazábal, J. Nazábal

Departamento de Ciencia y Tecnología de Polímeros and Instituto de Materiales Poliméricos "POLYMAT," Facultad de Ciencias Químicas UPV/EHU, P. O. Box 1072, 20080 San Sebastián, Spain

Received 24 April 2004; accepted 14 December 2004
DOI 10.1002/app.21789
Published online in Wiley InterScience (www.interscience.wiley.com).

ABSTRACT: Finely dispersed blends of polyamide 6 (PA-6) and poly(ethylene terephthalate) (PET) were obtained by direct injection molding throughout the full composition range. The blends comprised a probably pure PA-6 phase, and a PET phase that was apparently pure in PET-rich blends and contained slight reacted PA-6 amounts in PA-6-rich blends. This very complex morphology was characterized by the presence of dispersed particles at three levels and by a very large interface area/dispersed phase volume ratio. The linear ductility behavior was attributed to both the presence of reacted copolymers and the large interface area/dispersed volume ratio, and the synergism in both the Young's modulus and yield stress to the increased orientation of the blends related to that of the pure components. © 2005 Wiley Periodicals, Inc. J Appl Polym Sci 97: 564–574, 2005

Key words: polyamides; polyesters; blends; interchange reactions; compatibilization

INTRODUCTION

Polymer blends have been an attractive research subject for several decades.[1–4] It is also nowadays of great interest, as seen by both the increasing commercial use of polymer blends and the emergence of new research areas, such as compatibilizer addition and ternary polymer blends. Despite these new developments, the more traditional research field of binary polymer blends is still far from being fully exploited, both from the scientific and applied points of view. This is especially true in the case of specific research subjects such as, for instance, reactive processing and the compatibilization that it can lead to.

Among the very large number of polymer blends studied, the combination of a partially crystalline and an amorphous polymer is often studied, because their properties are often complementary. Binary blends of two crystalline polymers are, however, less frequent, the main reason being probably the complications that the interactions among the four phases of the blends may involve. Two of the most attractive semicrystalline polymers are polyamide-6 (PA-6) and poly(ethylene terephthalate) (PET). Despite their common semicrystalline nature, they have contrasting properties, as water sorption is very large in PA-6 and low in PET, and deflection temperature is low in PA-6 and high in PET.

Both PA-6 and PET have been blended with many second components. Among them, PA-6 has been blended with polyesters.[5–9] The PA-6/PBT blends showed[5–7] two T_g's. These blends were modified with either an epoxy resin,[5,8] phenoxy,[9] amorphous polyamide,[6] or 4,4′-biphenol[7] as compatibilizers. When epoxy was used, the copolymers formed[8] hindered the crystallization of both PA-6 and PBT. Both the impact strength[5] and the ductility[8] increases were very large while the modulus did not change.[8] The addition of phenoxy[9] to a 70/30 PA-6/PBT blend also led to reactions that increased tensile and impact properties and stabilized the morphology to annealing. The addition of amorphous polyamide[6] to a 30/70 PA-6/PBT blend led to a domain structure finer than that of the binary blend. The addition of 3 phr of amorphous polyamide led to a higher tensile modulus value, which decreased with increasing amorphous polyamide content. The addition of 4,4′-biphenol to a 40/60 PA-6/PBT blend also led to reactions that increased the tensile and flexural strengths, as well as the flexural modulus, and improved the compatibility as seen by SEM.

PET has been blended with polyamides other than PA-6.[10–17] The 15/85 PET/amorphous polyamide blend[10] was stated to be immiscible although the cooling sequence was not stated. The crystallization of PET in these blends has also been studied.[11] The blends of PET with PA-6,6 reacted in the melt state

Correspondence to: J. Nazábal (popnaetj@sq.ehu.es).

upon the addition of catalysts,[12–15] but showed brittle behavior.[12,14,16,17]

Binary PA-6/PET blends showed two amorphous phases when observed by DMTA,[18,19] but the position of the T_g's was not discussed[18] and did not change upon blending in the 50/50 blend.[19] The blends appeared miscible in the melt state, but crystallization led to phase separation of the components.[8,20] Upon drawing,[21] the increased orientation of the blends was attributed to highly oriented PET chains holding the PA-6 chains along their length. Reaction in the melt state led to the formation of copolymers.[18,20,22] Microfibrillar reinforced composites, with a PA-6 matrix and reinforcing oriented PET, were obtained; upon annealing at 240°C, a metastable miscible drawn 50/50 blend was obtained by ultraquenching.[22] Reactions were also observed[18,22] after annealing samples drawn at 240°C. Prolonged (25 h) annealing at 240°C of a 50/50 blend led to the complete incorporation of PA-6 in the copolymer, as shown by the disappearance of the glass transition peak of PA-6 by DMTA. WAXD showed that cocrystallization did not occur.[23] Compatibilization was reached[19] by means of the addition of at least 10–15 wt % Zn ionomer, and was attributed to both PA-6/ionomer association and PET/ionomer reactions.

Some mechanical properties of the drawn 50/50 blend,[22] before and after annealing, were measured. The quenched miscible blend was ductile, but ductility was lost, both on annealing induced phase separation[20] and on physical ageing.[19] Compatibilization with epoxy[23] improved both the flexural and notched impact strength of one blend. A quenched ductile 50/50 blend with a 15% Zn ionomer,[19] held at 25°C and R.H. 60%, retained its ductility for 1 month, but ductility decreased to 15% when the ionomer content was only 5%. Annealing, at 100°C during 30 min,[19] led to important ductility decreases (elongation at break of 4 and 15%, with 5 and 15% ionomer). The T_g's of the two pure components moved towards each other as a result of the addition of epoxy.[23] The brittle binary blends became ductile with only 10% phenoxy addition.

Thus, PA-6/PET blends, either drawn or annealed, as well as compatibilized, have been studied. However, the morphology, phase behavior, and mechanical properties have not been systematically studied and discussed. In this work, an attempt has been made to obtain PA-6/PET blends throughout the composition range by direct injection molding without previous extrusion mixing. The blends were characterized by means of DSC, DMTA, and SEM. Density was measured by displacement and orientation by ATR dichroism. Possible reactions were studied by FTIR. The observed phase structure and morphology were related to the mechanical properties measured by means of tensile tests. Annealing was also carried out to test the stability of both the structure and mechanical properties of the blends.

EXPERIMENTAL

Polyamide-6 (PA-6) (Durethan B30S) was supplied by Bayer. Its molecular weight was 29,000 as measured by viscometry at 25°C in a 85/15 formic acid/water solution. Poly(ethylene terephthalate) (PET) was supplied by Brilen (Barbastro, Huesca, Spain). It had an intrinsic viscosity of 0.82 dL/g in *o*-chlorophenol at 30°C. Both PET and PA-6 were dried for 14 h before processing, at 120°C in an air circulation oven, and at 100°C in a vacuum oven, respectively. Direct injection molding was carried out in a Battenfeld BA230E injection molding machine (screw diameter = 18 mm and L/D = 17.8) at a barrel and a nozzle temperature of 275°C, injection speed of 7.4 cm^3/s, injection pressure of 2650 bar, and mold temperature of 16°C. Direct injection molding improves the efficiency of the process, and avoids a prior extrusion-mixing process, which might contribute to degradation. The specimens were stored in a desiccator.

The thermal behavior of the blends and of the pure components was studied by differential scanning calorimetry (DSC) using a Perkin–Elmer DSC-7 calorimeter. The samples were heated from 20 to 280°C at 20°C/min. The crystallization and melting temperatures and heats were determined, respectively, at the maxima and from the areas of the corresponding peaks. The crystalline content of the blends could not be measured in the heating scans because the melting temperatures of PA (roughly 228°C) and PET (roughly 250°C) were very close. Therefore, it was measured in a fast cooling scan (50°C/min). The crystallinity of PET, in the pure state and in the blends, was also measured by X-ray diffraction (XRD). XRD patterns were recorded in a Philips PW 1729 GXRD X-ray diffractometer at 45 kV and 50 mA, using a Ni-filtered Cu-Kα radiation source. The scan speed was 0.5°/min. The phase structure of the blends was studied by dynamic mechanical analysis (DMTA) using a TA Instruments Q 800 DMA. For DMTA testing, additional drying was carried out for two days at 90°C in a vacuum oven. All the samples were heated from 0 to 150°C at a heating rate of 4°C/min and at a frequency of 1 Hz.

Possible chemical reactions between PA-6 and PET were studied by Fourier Transform infrared spectroscopy (FTIR) using a Nicolet Magna 560 spectrophotometer. An attenuated total reflection (ATR) objective attached to a Spectra Tech microscope and a mercury-cadmium telluride detector were used.

To measure the orientation, the tensile specimens were cut along the flow direction using a Leica 1600 microtome. Two measurements were carried out in three points of each specimen, as indicated in Figure 1.

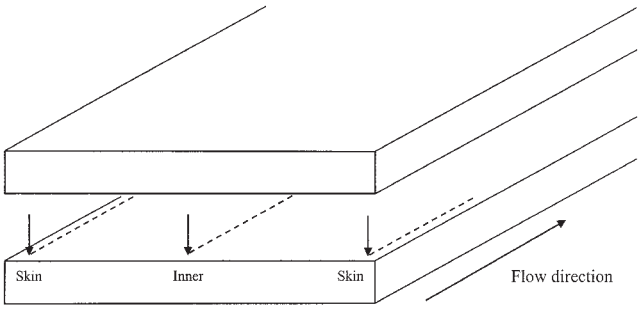

Figure 1 Schematic diagram of sample preparation and probe points for the orientation measurements.

The polarized ATR spectra were carried out at a 45° angle of incidence using a Nicolet Magna-IR 560 spectrophotometer equipped with an ATR accessory. The resolution was 8 cm^{-1} and each reported value is the average of the six points. The dichroic ratio D was the ratio of the intensities of the absorption bands of a characteristic group measured for parallel ($A_{\parallel}$) and perpendicular ($A\perp$) polarization with respect to the injection direction.

$$D = \frac{A_{\parallel}}{A_{\perp}} \tag{1}$$

The average orientation is expressed as the orientation parameter (f) that is related to the dichroic ratio as

$$f = \frac{(D-1)(D_0+2)}{(D+2)(D_0-1)} \tag{2}$$

where $D_0 = 2cot^2\alpha$, and α is the angle between the chain axis and the transition moment. Although α is not accurately known, 90° can be used as a first approximation for all the perpendicular bands, because this angle would give rise to the minimum orientation value.

Density was measured in a Mirage SD-120-L electronic densitometer (maximum typical deviation of 0.0008 cm^3/g), using butyl alcohol as immersion liquid.

The tensile tests were carried out using an Instron 4301 at a cross-head speed of 10 mm/min and at 23 ± 2°C on injected ASTM D-638 type IV (1.8 mm thick) specimens. The Young's modulus, E, and yield stress, σ_y, were determined from the load-elongation curves. The ductility was measured by means of the reduction of transversal area (d) by means of the expression:

$$d = \frac{A_0 - A}{A_0} \tag{3}$$

where d is the ductility, and A_0 and A are the initial and final transversal areas, respectively.

Izod impact tests (ASTM D-256) were carried out using a Ceast 6548/000 pendulum on injection-molded specimens. Notched (depth: 2.54 mm, radius: 0.25 mm) specimens machined after molding were tested. A minimum of eight specimens were tested for each reported value in both tensile and impact tests. To test the structural stability of the blends, annealing was carried out at 100°C for 30 min.

Scanning electron microscopy (SEM) was carried out on surfaces of cryogenically fractured specimens, after gold coating. A Hitachi S-2700 electron microscope was used at an accelerating voltage of 15 kV.

RESULTS AND DISCUSSION

Phase structure

The phase structure of the blends was studied by dynamic mechanical analysis (DMTA). Only one T_g was observed in the blends. However, the T_g peaks were very wide, indicating that, due to the proximity of the T_g's of the pure polymers, they probably corresponded to two overlapped T_g peaks. Thus, little information about the phase structure could be collected from the plots. However, it is known that PA-6 is very prone to pick humidity up; therefore, its T_g in the not fully dry state will slip towards lower temperatures. This effect is practically absent in PET due to its much smaller water uptake. These facts can be used to find whether two peaks are present in these blends, because the displacement of the T_g of the PA-6 will increase the difference between the two T_g's. For this reason, the blends were further tested by DMTA in a not fully dry state. The very different intensity of the peaks of pure PA-6 and PET hindered the observation of the plots of the PA-6-rich blends when all the scans were plotted together. For this reason, the log (tan δ) plots of neat PET and PET-rich blends are shown in Figure 2a, and the tan δ plots of neat PA-6 and PA-6-rich blends, in Figure 2b. The plot of the 50/50 blend is shown in both Figures as a reference.

As can be seen in Figure 2a, the maximum of the peak at high temperature, which must correspond to PET, appeared roughly at the same temperature as that of neat PET (84°C). This indicated the presence of a practically pure PET amorphous phase in the PET-rich blends. As can also be seen, and contrary to the behavior in dry blends, at low temperatures a slight shoulder was observed in the semilogarithmic plot, indicating the presence of another amorphous phase of obvious PA-6 nature. The positions of these shoulders and, as a consequence, the nature of the PA-6 phase, were difficult to determine, even on a semilogarithmic scale, and will be commented on later.

In Figure 2b, in both the 50/50 and the PA-6-rich blends, one peak at high temperature and clear shoulders appeared with all compositions. This is seen even

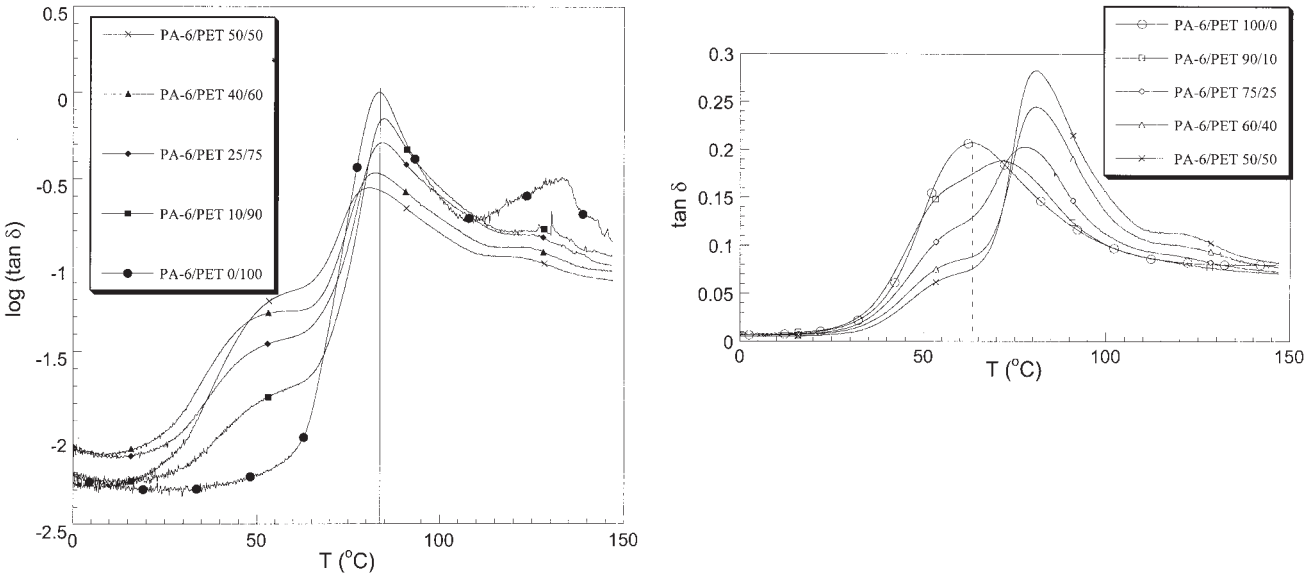

Figure 2 (a) Log (tan δ) versus temperature plot of the PET-rich blends, and (b) tan δ-T plot of the PA-6-rich blends.

in the blends very rich in PA-6, and is due to the very high intensity narrow peak of pure PET. The temperature at which the high temperature peak appeared also is below that of pure PET, mainly in the blends very rich in PA-6.

This slip of the high temperature T_g peak can be due to either a dilution effect, because of the presence of some mixed PA-6, or to a decrease in the crystallinity of PET in the presence of PA-6. The crystallinity of PET could not be measured in the heating scan because the melting temperatures of both polymers were very close, but it was the same in pure PET and in the blends in the cooling scan. Therefore, a change in crystallinity was not the reason for the observed T_g decrease. As a consequence, the presence of slight PA-6 content mixed in the PET-rich phase of the PA-6 rich blends is proposed.

In Figure 2b, clear shoulders also were observed at low temperatures, indicating the presence of a PA phase. As in the case of Figure 2a, the positions of the corresponding peaks are difficult to locate accurately. However, they appear to be below the T_g of PA-6 (63°C). In the tan δ scan of the twice dried blends, the position of the shoulder was closer to that of PA-6 (roughly 77°C), but the position of the corresponding T_g peak was also uncertain. The position of the T_g of the PA-6, which leads to the shoulder at low temperature, can also be studied by means of the position of the first derivative of the tan δ plot. This is because the maximum of the first derivative in the heating side of the peak appears at lower temperature than the T_g, so it will barely be affected by the high temperature peak of PET. The position of the maximum of the first derivative peak in the blends, which indicates the position of the inflection point, did not change with composition, and was very similar to that of PA-6 (47°C). This points to the presence of a rather pure PA-6 amorphous phase in the blends, but a presence of slight PET amounts in the PA-6-rich phase cannot be discarded. A lack of change in the T_g's upon melt mixing in a mini-molder at 280°C for 5 min was stated,[24] but the T_g's were studied by DSC, which is a technique clearly less sensitive than DMTA to small T_g changes. Although no attention was paid to a possible T_g change, copolymers[20,22] were observed upon annealing of a 50/50 PET/PA-6 blend at only 240°C for 25 h. The presence of copolymers should change the T_g and will be discussed in the next paragraph.

The PA-6 in the PET amorphous phase can be either miscibilized or reacted, or both. To prove if reactions took place, the carbonyl region of the FTIR spectra of the PA-6/PET 75/25, 50/50, and 25/75 blends are compared with those obtained from the weighted addition of the spectra of the pure PA-6 and PET in Figures 3a–c, respectively. In the experimental spectra of the 50/50 and 25/75 blends (Figs. 3b and 3c), the bands of the carbonyl group of both PET and PA-6 (at 1711 and 1631 cm^{-1}, respectively) were displaced. In the 75/25 blend (Fig. 3a), the band of the carbonyl group of PET moved, but that of PA-6 did not. These displacements could be a consequence of either intermolecular interactions between PET and PA-6 or the existence of chemical reactions. To elucidate which possibility occurred, the ^{1}H-NMR spectrum of the injection molded PA-6/PET (50/50) blend and also that of a 50/50 mixture of pellets of the components as a reference were performed and are collected in Figure 4. Some new peaks were observed in the spectrum of the injection molded blend in the region between $\delta = 1.0$ and $\delta = 2.0$ ppm approximately. Although of

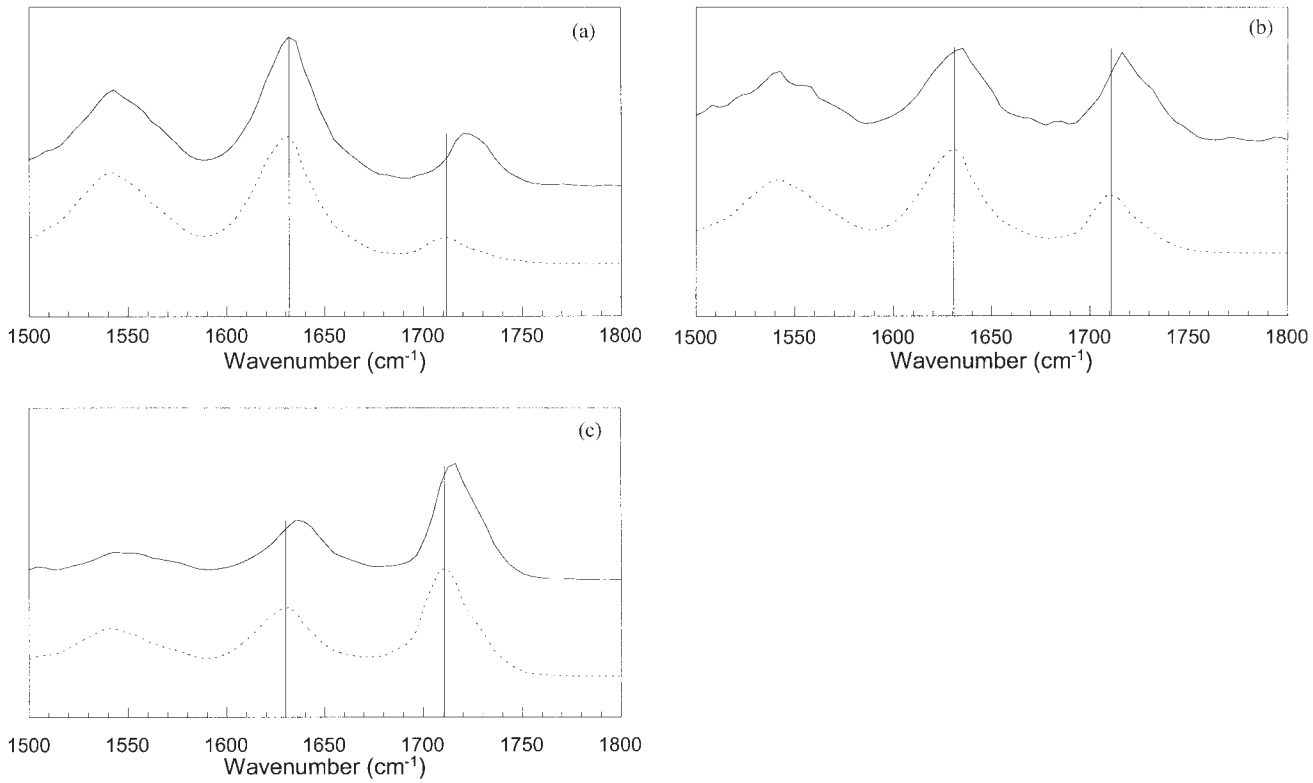

Figure 3 Experimental (−) and calculated (- - -) FTIR spectra of the (a) 75/25, (b) 50/50, and (c) 25/75 blends.

smaller intensity, these signals were similar to those found in the same blend after 2 h reactive blending at 280°C.[25] Therefore, although the occurrence of H-bonding cannot be discarded, the observed FTIR and NMR peaks indicate the occurrence of reactions. As can also be seen in the FTIR spectra of Figure 3, the displacement of the carbonyl group of PET increased with the PA-6 content. This is in agreement with DMTA data because the displacement of the tan δ peak of PET increased with the PA-6 content. This displacement of the tan δ peak rules out a possible H-bonding effect, and indicates that the reaction was more pronounced at higher PA-6 contents. The decrease in the displacement of the PA-6 peak (at 1631 cm^{-1}) at higher PA-6 contents is attributed to the relative decrease in the amount of reacted PA-6. The disappearance of the T_g of the PA-6 after large reaction extents[18] has been reported. Therefore, the copolymer

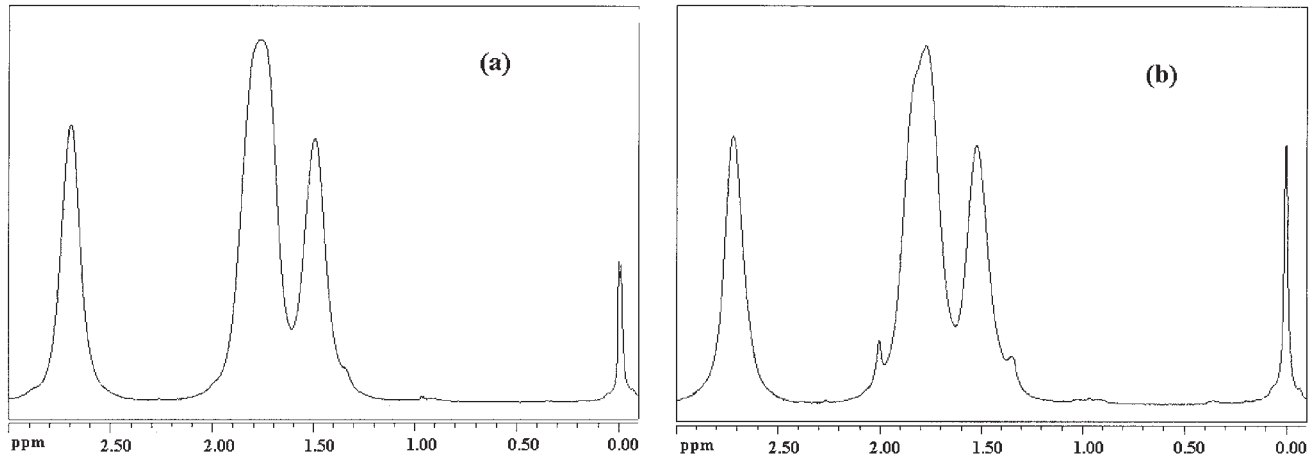

Figure 4 ^{1}H-NMR spectra of (a) a 50/50 mixture of PA-6 and PET pellets and of (b) an injection molded PA-6/PET (50/50) blend.

migrated to the PET-rich phase. This agrees with the slip of the log (tan δ) peak of the PET-rich phase towards lower temperatures observed in the DMTA scans. Both the observed band and the T_g displacements were slight, indicating a low reaction extent. As a consequence, the slight changes of the T_g of the PET-rich phase are not attributed to partial miscibility, but to the presence of reacted copolymers.

The crystalline characteristics of both PET and PA-6 were studied by DSC. With respect to the crystalline phase of PET, pure PET and most of the blends presented a crystallization exotherm in the first DSC heating scan, indicating that PET did not fully crystallize after molding. The crystallization temperature of PET (roughly 140°C) decreased to 111°C with the addition of PA-6, indicating that PA-6 facilitated the crystallization of PET. A nucleation effect was also observed in the cooling scan, and in PA-6/PET,[21,22] PET/PA-6,6,[13,16,26] and PET/amorphous polyamide[10] blends. The melting temperature of PET decreased slightly (roughly 5°C) with the addition of PA-6.

In the heating scan, the crystallinity of PET was close to 6%. That of the blends could not be measured because, as stated before, the T_m of both PET and PA were very close. To investigate further the crystallinity of PET in the blends, pure PET and the 50/50 blend were cooled in the calorimeter after the heating scan at the maximum cooling temperature (50°C/min) at which any crystallization peak could be measured. The crystalline contents were, respectively, 20 and 16%. This difference is not significant as it is similar to the expected experimental error; therefore, the presence of PA-6 did not significantly affect the crystallinity of PET in the cooling scan. This suggests that, after injection molding, the crystallinity content of PET in the blends was also similar to that of pure PET (6%). When the crystalline contents were measured by XRD, the results, although less accurate than those of DSC, were in agreement with those obtained by DSC. This lack of effect of the presence of PA-6 in the crystalline content of PET agrees with that observed in PET/PA-6[20,22] and PET/amorphous polyamide[11] blends. However, PET crystallinity increased in another study of blends of PET with the same amorphous polyamide[10] and in PET/PA-6,6 blends with[13,14] and without[14,16] the addition of catalyst.

With respect to the crystalline phase of PA-6, the melting temperature decreased. The crystallization temperature, during cooling, remained constant with the addition of PET, indicating that PET did not influence the crystallization of PA-6. However, PBT promoted the crystallization of PA-6.[8] In agreement with previous works,[20,22] the crystallinity of PA-6 (roughly 35%) remained practically constant in the blends of this study. However, increases in the crystallinity of PA-6[21] were seen in PA-6/PET fibers; they were attributed to the presence of highly oriented PET chains, which act as nuclei for the formation of PA-6 crystals.[21]

Morphology

The morphologies of the cryogenically broken surfaces of the PET/PA-6 90/10, 75/25, 60/40, 40/60, and 25/75 blends are shown, respectively, in Figures 5a–e. Details of the morphology of the 60/40 and 25/75 blends are shown, respectively, in Figures 5f and 5g. The morphology of the 50/50 blend was intermediate between those of the 60/40 and 40/60 compositions. As can be seen in Figure 5a, the morphology was mostly homogeneous, with a dispersed particle size usually below 0.6 μm. This indicated that direct injection mixing is an adequate procedure to obtain these blends. Even taking into account the low PET content, the particle size was small, leading to a large contact surface/volume ratio of the dispersed phase, which indicated that the interfacial tension was low.

In the 75/25 blend of Figure 5b, surprisingly, the size of most of the dispersed spherical PET particles was smaller (mostly close to 0.2 μm) than in the 90/10 blend. This is attributed to the presence of large (typically 2 μm) broken particles with no very clear boundaries and with some smaller PA-6 particles inside. Such large particles were only sporadic in the 90/10 blend. The morphology was less homogeneous in this composition; as in the zones with lower presence of large particles, the dispersed particle size increased. This complex salami-like structure implies an even larger contact surface than in the usually simple particles, and corroborates the low interfacial tension of the blends. A low interfacial tension confirms the chemical reactions that were seen by FTIR. No similar structure has been detected previously, to our knowledge, in PA-6/PET blends.

As can be seen in Figure 5c for the 60/40 blend, the dispersed particle size is at least as fine as in Figure 5b. This is despite the larger PET content, and comes with more frequent presence of large particles. A detail of this composition is shown in Figure 5f. The presence of small (typically 0.3 μm) particles of obvious PA-6 nature inside the PET dispersed phase is clear. As can also be seen, particles as small as 0.5 μm are broken. This is a low value because the interfacial adhesion must be high to reach the fracture strength in such a small contact surface. It also indicates that, as some reaction occurred in the blends of this study, compatibilization will probably not be necessary. Particles smaller than 0.5 μm are mostly debonded, both in the matrix and inside the PET dispersed phase.

In the 40/60 blend of Figure 5d, the dispersed phase size increased with respect to that of Figure 5c, and the large particles occupied almost half the fracture surface. Moreover, the morphology of this blend was more similar to that of PA-6-rich blends than to the

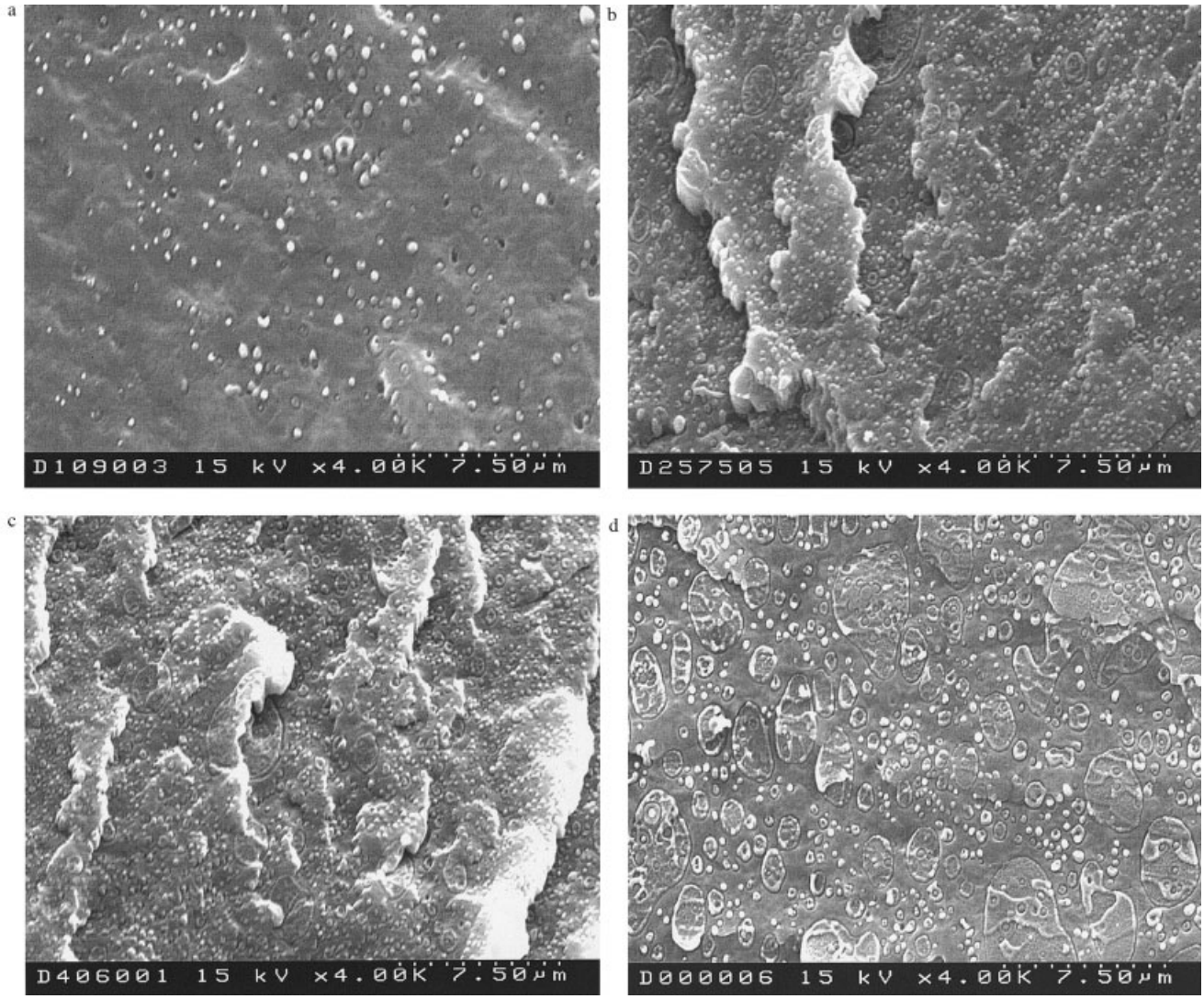

Figure 5 Morphology of the cryogenically broken surfaces of the (a) 90/10, (b) 75/25, (c) 60/40, (d) 40/60, and (e) 25/75 blends, and of the (f) 60/40 and (g) 25/75 blends at high magnification. The photographs were obtained by SEM at an angle of 30° from the perpendicular to the surface.

rest of the PET-rich blends, indicating that the matrix still had a PA-6 nature and that phase inversion had not taken place. The PA-6 matrix nature of this blend is unexpected, and should be related to the viscosity ratio of the components. Therefore, the viscosities of both PA-6 and PET were measured by means of the torque of mixing, which is known[27] to be related to viscosity. The melt torques of PA-6 and PET were at 275°C and 30 rpm 0.8 Nm, and 1.63 Nm, respectively. The composition at which cocontinuous phases would be expected is given by the equation:[27]

$$\frac{\eta_1\phi_2}{\eta_2\phi_1} \cong 1 \qquad (4)$$

where η_1 and η_2 are the viscosities of PA-6 and PET, respectively, and ϕ_1 and ϕ_2 are the volume fractions. Substituting the melt torques in eq (4), the phase inversion should occur at $\phi_1 = 0.33$ (29 wt % PA-6 content); thus, at a PA-6 content below 40%, in agreement with the SEM observations.

Figure 5e shows the morphology changed in the 25/75 blend, indicating that phase inversion took place between 40 and 25% PA-6 content. Most particles were debonded, and only particles larger than roughly 2 μm appeared broken. The presence of complex structures, such as those found in the rest of the blends, was rare. Residues of bound matrix appeared on the surface of some dispersed particles. A detail of the complex particle morphology is seen in Figure 5g. The morphology is really complex, with three dispersed particles types: large particles (maximum size 5 μm), occlusions (maximum size 3 μm), and small particles (typically 0.5 μm) inside the occlusions.

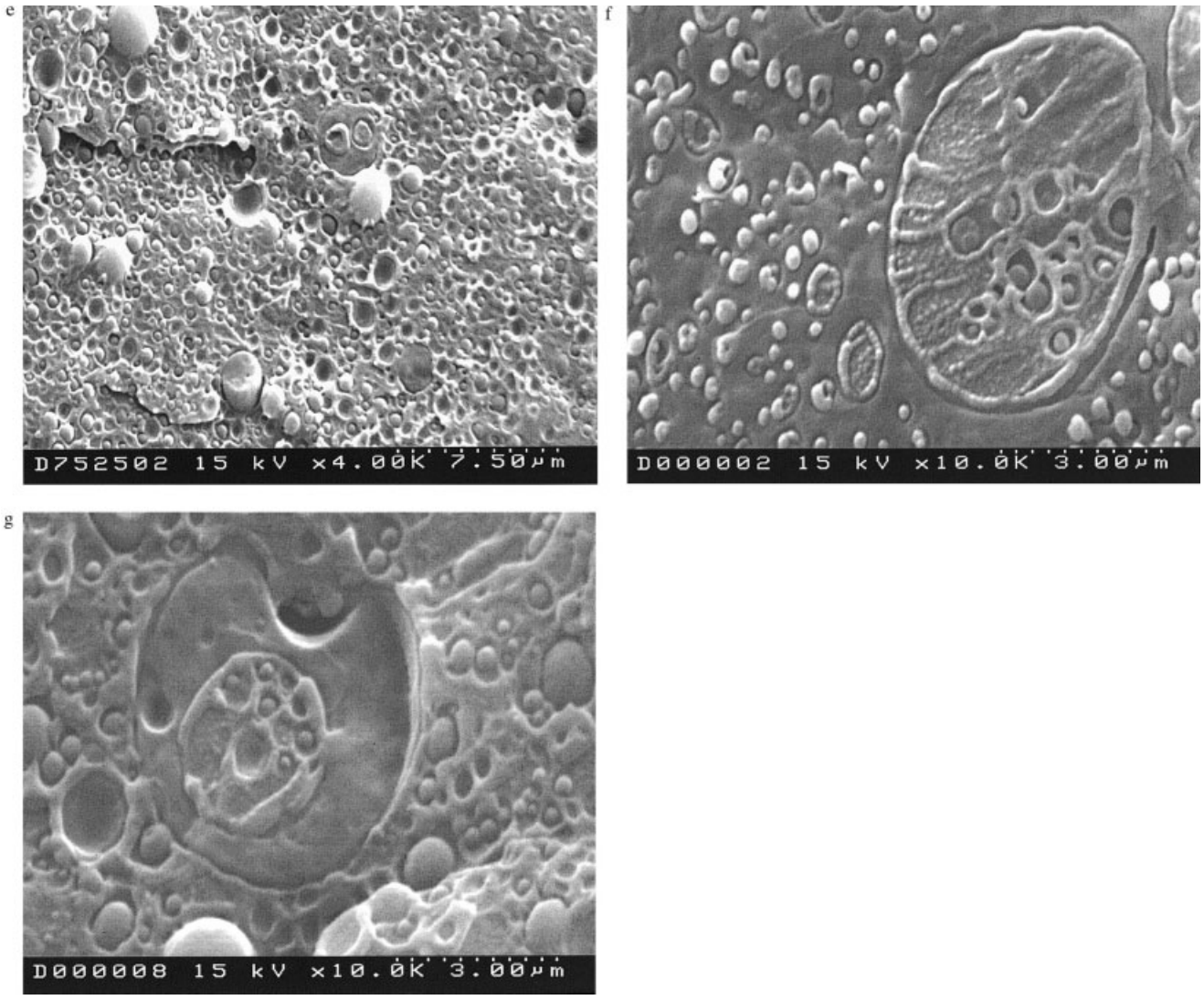

Figure 5 (*Continued from the previous page*)

The morphology of the 10/90 blend was similar to that of the 25/75 blend. As expected, the particle size decreased. No large particles were seen in the homogeneous structure of this composition.

Mechanical properties

The moduli of elasticity of the blends versus composition are shown in Figure 6. The best approximation to the experimental values is drawn as a continuous line, the modified rule of mixtures is indicated by a series of points, and the reference single rule of mixtures appears as a broken line.

Modulus behavior is synergistic with all the compositions studied, and the modulus values always lie above those predicted by the rule of mixtures. The synergism is absolute in at least the 90/10 composition, and values very close to those of the pure PA-6 appear both in the 75/25 and 60/40 blends, despite the smaller modulus of PET compared with that of PA-6. The occurrence of modulus values above those predicted by the rule of mixtures is not an unusual behavior in polymer blends as it often takes place both

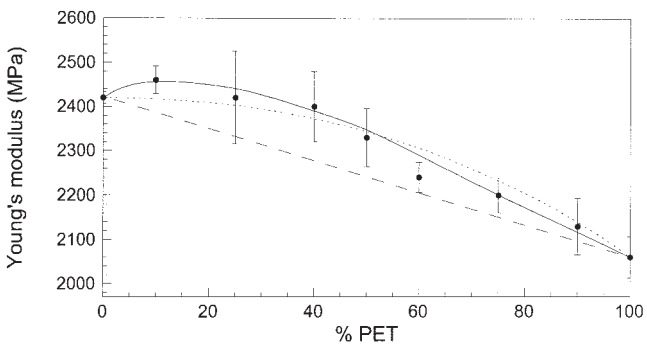

Figure 6 Moduli of elasticity of the blends against composition. The dotted curve represents the modified law of mixtures, the discontinuous straight line the rule of mixtures, and the continuous curve the best fit to the experimental values.

TABLE I
Orientation Parameter of the Blends Measured by FTIR

Composition of the blend	100/0	75/25	50/50	25/75	0/100
Orientation parameter	0	0.056	0.047	0.036	0.036

in miscible[28–30] and in immiscible[31,32] blends. It can also take place in incompatible blends, as incompatibility is seen in fracture properties in which the lack of adhesion is clear. The modulus behavior is often predicted by the modified rule of mixtures proposed by Nielsen:[33]

$$E = E_1\phi_1 + E_2\phi_2 + \beta_{12}\phi_1\phi_2 \quad (5)$$

where E and ϕ are the modulus and the volume fraction, respectively, the subscripts 1 and 2 refer to the two components of the blend, and β_{12} is an empirical parameter that can be calculated as

$$\beta_{12} = 4\,E_{12} - 2E_1 - 2\,E_2 \quad (6)$$

where E_{12} is the modulus of the 50/50 blend.

As can be seen, the experimental values are only partially depicted by this rule. This is because the predicted behavior is based, besides on the modulus of the pure components, only on the value of the 50/50 blend. This leads to a symmetric shape with respect to the 50/50 composition, while the deviations of the experimental values from linearity are different in PA-6-rich and PET-rich blends. It is known that the β_{12} coefficient measures the importance of the synergism. For this reason, it will be used to compare this synergism with that of other blends. Thus, the β_{12} coefficient obtained in this study (360 MPa) is smaller but comparable to that obtained in miscible blends, such as poly(2,6-dimethyl-1,4-phenylene oxide) (PPO)/poly(styrene-*co*-*p*-chlorostyrene) (β_{12} = 660 MPa).[34]

As the crystallinity level of both PET and PA-6 did not change on blending, and the reactions cannot produce grafted products (due to the chemical structure of the components of the blend), the deviation of the modulus values with respect to linearity upon blending should be due to changes of either free volume due to hydrogen bonding, or orientation in the components of the blends. For this reason, both the density and the orientation of the blends and of the pure components were measured. The density values are representative of the free volume of the amorphous phases, as the crystallinity of both the PA-6 and PET was the same both in the pure components and in the blends. The density values were close to linear; therefore, a change of density upon blending is not the reason for the observed synergism in the modulus of elasticity.

The orientation parameter of some blends and the pure components is collected in Table I. As can be seen, the orientation of the blends is not only synergistic, but is generally higher than that of either of the two pure components. Moreover, the highest values appeared in the PA-6-rich blends, where the positive deviation of the modulus was the highest. This indicated that the observed synergism in the moduli of elasticity of the blends was due to higher orientation of the components in the blends than in the neat state.

The yield stress of the blends is plotted in Figure 7 against composition. As can be seen, the behavior of the yield stress is synergistic, with absolute synergy both in the 90/10 and 75/25 compositions. This behavior is very similar to that observed in the modulus of elasticity, as often seen in polymer blends,[35] despite the different deformation level at which both properties are measured. The notched impact strengths of the blends versus composition are shown in Figure 8. As can be seen, the overall values are either similar to or below that of pure PET. This is usual in compatibilized polymer blends without any rubber modification, indicating that the dispersed phase is not able to change the fracture characteristics of the matrix at the high strain rate associated with the impact tests.

The ductility of the blends was measured by means of both the reduction of the cross section and the elongation to fracture. When specimens break in the tensile tests during cold drawing, as in this study, large differences in elongation at break do not indicate large differences in ductility. The values of the reduction in the cross section are more representative of ductility and are plotted versus composition in Figure 9. As was seen when ductility was measured by means of the elongation at fracture, the ductility values of the

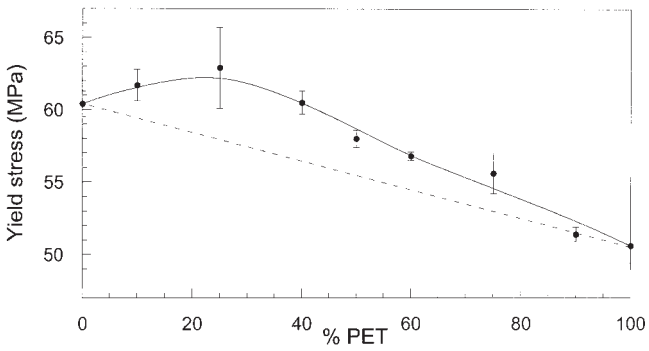

Figure 7 Yield stress of the blends against composition.

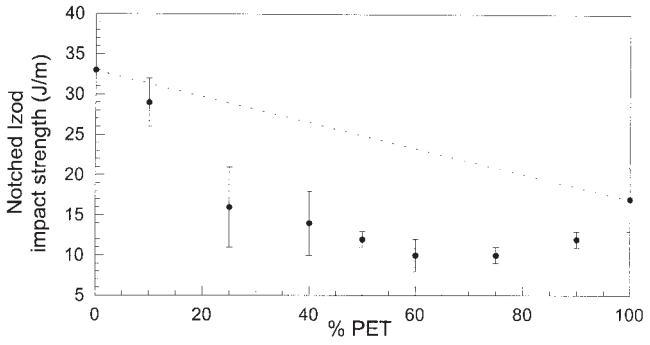

Figure 8 Notched impact strength of the blends against composition.

blends were very similar to those of the pure components. This is very unusual in almost immiscible blends, and is a clear indication both of the compatibilizing effect of the produced copolymers and the very positive effect on ductility of structures with a large interface area/dispersed phase volume ratio, such as the either small or complex morphologies of these PA-6/PET blends. Moreover, compatibilization was attained with a very small amount of reacted products, as seen by the very slight T_g change. This is an important difference between small T_g changes due to either partial miscibility or reaction. In the case of reaction, the minority component locates at the interface, leading to a relevant effect. In the case of miscibility, the same amount is distributed across the phase, leading to a greatly reduced effect.

Good mechanical properties were also seen in PA-6/PET drawn blends.[22] They could be due to the physical interlocking of components when PA-6 melt penetrates the initially crystallized PET at their interface during melt cooling, as suggested in PA-6,6/PET blends.[1] Also, the higher expansion coefficient of PA-6 (2.40×10^{-4}°C^{-1}) compared with that of PET (1.95×10^{-4}°C^{-1}) must lead to PA-6 contracting more during cooling. This should help adhesion when PA-6 is the matrix, but lead to debonding when it is PET.[19] In these blends, neither drawing nor bad properties, when PET is the matrix, appeared, indicating that compatibilization by reaction was the reason for the observed positive fracture behavior.

A good ductility value was obtained in a quenched miscible 50/50 PA-6/PET blend[22] due to its highly amorphous state. However, the blend embrittled upon crystallization during annealing. Good ductility values of quenched PA-6/PET 50/50 blends also drastically decreased after annealing for half an hour at 100°C (from 396 to 7%) even when an ionomer was added[19] due to the crystallization of PET during annealing. In the case of the blends of this study, quenching was not carried out. However, to test the thermal stability of the structures obtained, the 75/25 and 25/75 blends were also annealed for half an hour at 100°C in a vacuum oven. The crystallization peak of PET in the unannealed blends disappeared upon annealing, indicating that PET was fully crystallized in the annealed blends. However, the blends remained ductile as they broke in the cold drawing region (elongation at break 132 and 33% for the 75/25 and 25/75 blends, respectively). This difference in ductility between the annealed blends of this study and those of the previous study[19] is attributed to the different crystalline structure of PET, as in this study PET crystallized from the melt and in an oriented condition. This is in contrast to the crystallization of a quenched unoriented PET during annealing, where even the neat PET may appear brittle.[14]

CONCLUSIONS

Homogeneous PA-6/PET blends, with a large interface area at all blend compositions, were obtained by direct injection molding. The blends were composed of a probably pure PA-6 amorphous phase, and a PET phase that had small amounts of PA-6 in the PA-6-rich blends, and was apparently pure in PET-rich blends. The blend components reacted slightly during processing as seen by FTIR. This decreased interfacial tension, and led to an intimately mixed blend, with dispersed particles at three different levels and a very large interface area/dispersed phase volume ratio that would have aided the stress transmission through the interface.

The mechanical properties of the blends were advantageous. This was because general synergy was obtained in both the modulus of elasticity and the yield stress due to the larger orientation in the blends than in the pure components. Moreover, the ductility of the blends was similar to that of the components. This was attributed to both the presence of copolymers and to the very large interface area/dispersed phase volume ratio observed in these blends. The ductile nature of both the 75/25 and 25/75 blends was maintained after annealing at 100°C for half an hour,

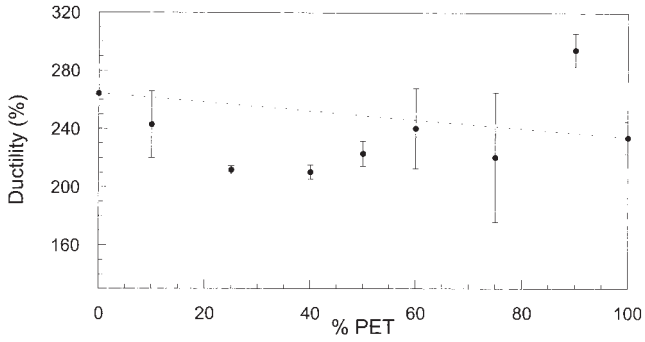

Figure 9 Ductility of the blends, measured by means of the area reduction of the cross section, against composition.

showing the thermal stability of the obtained morphologies.

The financial support of the Spanish "Ministerio de Educación y Cultura" (Project No. MAT2000–1742) is gratefully acknowledged. A. Retolaza also acknowledges the University of the Basque Country for the award of a grant for the development of this work.

References

1. Utracki, L. A. Polymer Alloys and Blends: Thermodynamics and Rheology; Hanser: Munich, 1989.
2. Paul, D. R.; Bucknall, C. B. Polymer Blends: Formulation and Performance; Wiley-Interscience: New York, 2000.
3. Paul, D. R.; Newman, S. Polymer Blends; Academic Press: London, 1978.
4. Shonaike, G. O.; Simon, G. P. Polymer Blends and Alloys; Marcel Dekker: New York, 1999.
5. An, J.; Ge, J.; Liu, Y. J Appl Polym Sci 1996, 60, 1803.
6. Kang, T. K.; Kim, Y.; Cho, W. J.; Ha, C. S. Polym Eng Sci 1996, 36, 2525.
7. Xiaochuan, Z.; Shibata, M.; Yosomiya, R. Polym Polym Compos 1997, 5, 501.
8. Chiou, K. C.; Chang, F. C. J Polym Sci, Part B: Polym Phys 2000, 38, 23.
9. Dharaiya, D.; Jana, S. C.; Shafi, A. Polym Eng Sci 2003, 43, 580.
10. Nadkarni, V. M.; Shingankuli, V. L.; Jog, J. P. Polym Eng Sci 1988, 28, 1326.
11. Nadkarni, V. M.; Shingankuli, V. L.; Jog, J. P. J Appl Polym Sci 1992, 46, 339.
12. Pillon, L. Z.; Utracki, L. A. Polym Eng Sci 1984, 24, 1300.
13. Pillon, L. Z.; Utracki, L. A. Polym Proc Eng 1986, 4, 375.
14. Pillon, L. Z.; Lara, J.; Pillon, D. W. Polym Eng Sci 1987, 27, 984.
15. Pillon, L. Z.; Utracki, L. A.; Pillon, D. W. Polym Eng Sci 1987, 27, 562.
16. Kamal, M. R.; Sahto, M. A.; Utracki, L. A. Polym Eng Sci 1982, 22, 1127.
17. Kamal, M. R.; Sahto, M. A.; Utracki, L. A. Polym Eng Sci 1983, 23, 637.
18. Serhatkulu, T.; Erman, B.; Bahar, I.; Fakirov, S.; Evstatiev, M.; Sapundjieva, D. Polymer 1995, 36, 2371.
19. Samios, C. K.; Kalfoglou, N. K. Polymer 1999, 40, 4811.
20. Evstatiev, M.; Fakirov, S. Polym Networks Blends 1994, 4, 25.
21. Varma, D. S.; Dhar, V. K. J Appl Polym Sci 1987, 33, 1103.
22. Fakirov, S.; Evstatiev, M.; Schultz, J. M. Polymer 1993, 34, 4669.
23. Huang, Y.; Liu, Y.; Zhao, C. J Appl Polym Sci 1998, 69, 1505.
24. Lee, M. S.; Ha, M. G.; Choi, C. N.; Yang, K. S.; Kim, J. B.; Kim, T. H.; Choi, G. D. Polym J 2002, 34, 510.
25. Denchev, Z.; Kricheldorf, H. R.; Fakirov, S. Macromol Chem Phys 2001, 202, 574.
26. Retolaza, A.; Eguiazábal, J. I.; Nazábal, J. Polym Eng Sci 2004, 44, 1405.
27. Jordhamo, G. M.; Manson, J. A.; Sperling, L. H. Polym Eng Sci 1986, 26, 517.
28. Avramova, N. Polymer 1995, 36, 801.
29. Kleiner, L. W.; Karasz, F. E.; Macknight, W. J. Polym Eng Sci 1979, 19, 519.
30. Joseph, E. A.; Lorenz, M. D.; Barlow, J. W.; Paul, D. R. Polymer 1982, 23, 112.
31. Erro, R.; Gaztelumendi, M.; Nazábal, J. J Polym Sci, Part B: Polym Phys 1996, 34, 1055.
32. Jurado, M. J.; Gaztelumendi, M.; Nazábal, J.; Mondragón, I. J Polym Sci, Part B: Polym Phys 1990, 28, 1015.
33. Nielsen, L. E. Predicting the Properties of Mixtures; Marcel Dekker: New York, 1978.
34. Fried, J. R.; MacKnight, W. J.; Karasz, F. E. J Appl Phys 1979, 50, 6052.
35. Brown, N. In Failure of Plastics; Brostow, W.; Corneliussen, R. D., Eds.; Hanser Publishers: Munich, 1986; Chapter 6.